SECTION 4
LITERATURE REVIEW

INTRODUCTION

This review of the literature is divided into three parts. In the first section the characteristics of limestone are discussed. Limestone is, in most parts of the country, a readily available and inexpensive source of $CaCO_3$. However because it is a natural material, its physical and chemical characteristics are variable and this variability may affect its use as a neutralizing substance.

The engineering design of a limestone contactor requires an understanding of the kinetics of the neutralization ($CaCO_3$ dissolution) reaction. This topic is covered in the second part of the literature review.

In the third part of the literature review the effect of water chemistry on the release of corrosion by-products such as lead from lead-tin solder and copper from copper pipes is discussed.

LIMESTONE PROPERTIES

Limestone is a general term used to describe sedimentary rock composed primarily of calcium carbonate or combinations of calcium and magnesium carbonate with varying amounts of impurities, the most common of which are silica and alumina. There are numerous forms and types of limestone, varying in chemical composition, mineralogy, crystallinity, color, texture and hardness. Next to sand and gravel, limestone, including all of its carbonate forms, is the second greatest tonnage material produced in the United States.

The two most fundamental types of limestone are high calcium and dolomitic limestone. Pure high calcium limestone is 100 percent calcium carbonate (calcite or aragonite). Pure dolomite is 54.3% $CaCO_3$ and 45.7% $MgCO_3$. High-quality, high calcium limestone is 97-99% $CaCO_3$. (54-56% CaO). Chemical analyses for a number of U.S. limestones are summarized in Table 1.

High calcium limestone was used exclusively in this study. Since there is considerable evidence to suggest that the dissolution rate of dolomitic limestone is substantially less than high calcium limestone (Pearson and McDonnell 1975a, 1975b) the results of this study should therefore, only

Table 1 Representative chemical analyses (percentage composition) of different types of limestone (from Boynton, 1980)

	Limestone Sample*							
	1	2	3	4	5	6	7	8
CaO	54.54	38.90	41.84	31.20	29.45	45.65	55.28	52.48
MgO	0.59	2.72	1.94	20.45	21.12	7.07	0.46	0.59
CO_2	42.90	33.10	32.94	47.87	46.15	43.60	43.73	41.85
SiO_2	0.70	19.82	13.44	0.11	0.14	2.55	0.42	2.38
Al_2O_3	0.68	5.40	4.55	0.30	0.04	0.23	0.13	1.57
Fe_2O_3*	0.08	1.60	0.56	0.19	0.10	0.20	0.05	0.56
SO_3	0.31	--	0.33	--	--	0.33	0.01	--
P_2O_5	--	--	0.22	--	0.05	0.04	--	--
Na_2O	0.16	--	0.31	0.06	0.01	0.04	--	--
K_2O	--	--	0.72	--	0.01	0.03	--	--
H_2O	--	--	1.55	--	0.16	0.23	--	n.d.
Other	--	--	0.29	--	0.01	0.06	0.08	0.20

*

1 = Indiana high calcium stone.

2 = Lehigh Valley, Pa. "cement rock."

3 = Pennsylvania "cement rock."

4 = Illinois Niagaran dolomitic stone.

5 = Northwestern Ohio Niagaran dolomitic stone.

6 = New York magnesium stone.

7 = Virginia high calcium stone.

8 = Kansas cretaceous high calcium (chalk).

be applied to the use of high calcium stone. Active sources (quarries and mines) of high calcium limestone are present in essentially every state (See Figure 1).

Care must be taken in selecting a high calcium stone for use in a limestone contactor. Some states have either high calcium or dolomitic or abundant quantities of both types. The distribution of these materials is however without a predictable pattern, in some cases they occur in separate broad expanses, while in other cases both types may be present in close proximity, for example, on opposite sides of a quarry.

Limestone may contain a number of impurities. Clay, silt and sand (or other forms of silica) may have become incorporated in the stone when it was first deposited or material may have collected later in crevices and between strata. These mineral contaminants are the sources of the major impurities, silica and alumina. Other impurities, in a rough order of relative amounts are iron, phosphorus and sulfur. Trace substances such as manganese, copper, titanium, sodium, potassium, fluorine, arsenic and strontium may be present.

Murray et al. (1954) analyzed 45 different high calcium limestones from the United States. The principal impurities are listed in Table 2. All stone analyzed contained measurable amounts of silica, alumina and magnesium oxide. Potassium, sodium and sulfur were present in some samples.

Murray et al. (1954) also examined 25 high calcium limestones spectrographically for 25 metallic elements. The findings obtained for elements other than calcium, magnesium, silicon and iron are listed in Table 3. Aluminum, barium, manganese,phosphorus, potassium, sodium, strontium and tin were detected in all 25 samples. Titanium, zinc and chromium were detected in 20 of the samples. The metals present at a concentration greater than 1000 ppm in at least one sample are aluminum, manganese, potassium, sodium, strontium, titanium and zinc.

KINETICS OF LIMESTONE DISSOLUTION

The engineering design of a limestone contactor requires an understanding of the kinetics of the $CaCO_3$ dissolution process and the effect of this dissolution on the chemistry of the bulk solution. The overall neutralization/dissolution reaction is given by

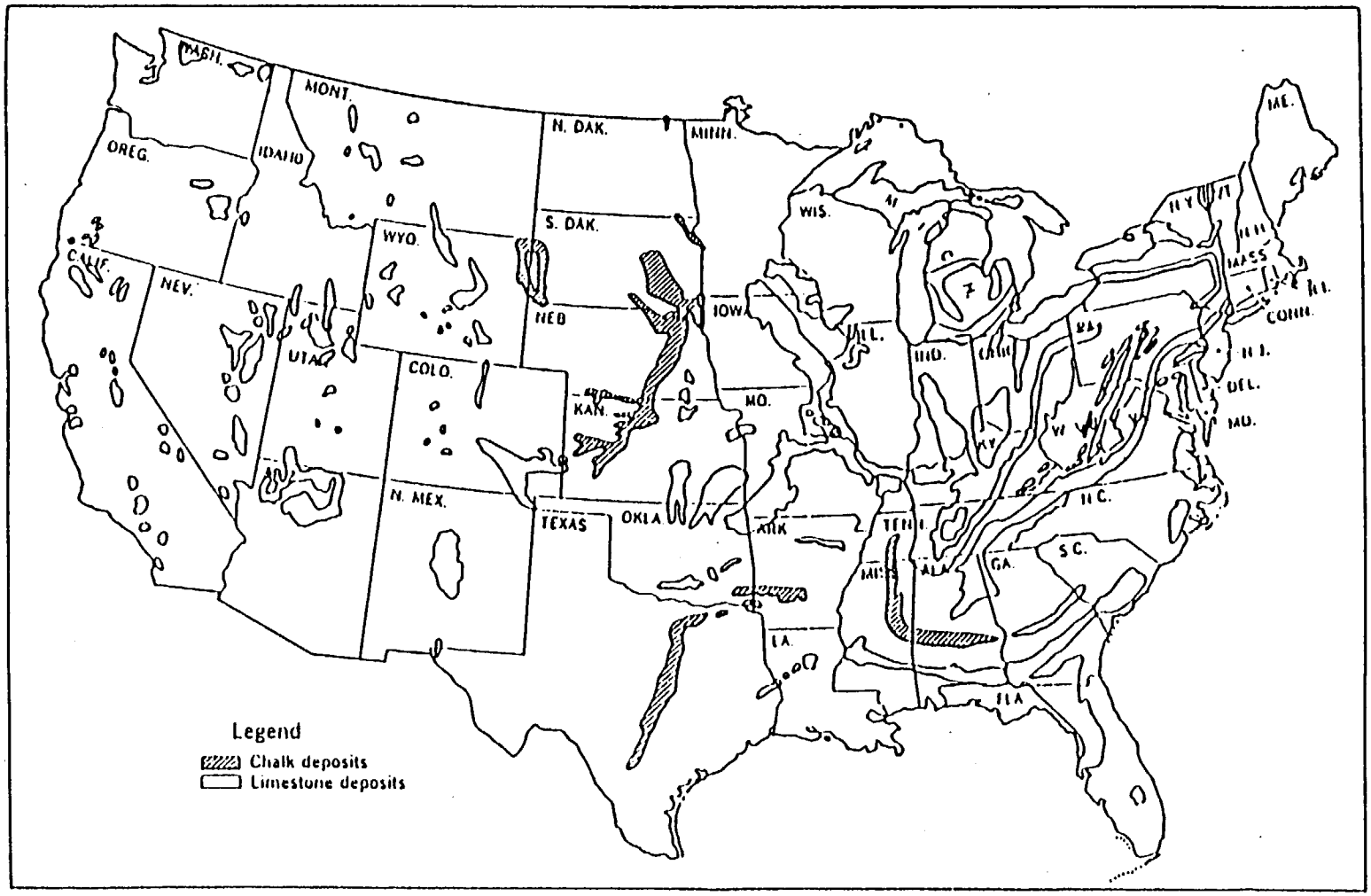

Figure 1. Locations of major chalk and limestone deposits in the continental United States.

Table 2 Major Impurities in High Calcium Limestone (45 U.S. Samples) (from Murray et al., 1954)

SiO_2	0.10 - 2.89%
Al_2O_3	0.13 - 0.92%
K_2O	0.00 - 0.21%
Na_2O	0.00 - 0.16%
SO_3	0.00 - 0.56%
MgO	0.12 - 3.11%

Table 3 Minor Impurities in High Calcium Limestone (25 U.S. Samples) (from Murray et al., 1954)

Element	Number of Samples With Detectable Amount	Maximum Amount
Al	25	0.35-0.60% (5 samples)
Ba	25	not given
B	3*	
Cr	20	10 ppm+ (3 samples)
Co	9	10 ppm+ (2 samples
Pb	15*	
Mn	25	0.1%+ (1 sample)
Hg	4	
Mo	8*	
Ni	22	0.01% (1 sample)
P	25	0.001-0.01% (2 samples)
K	25	0.2% (1 sample)
Ru	17*	
Ag	13*	
Na	25	0.1%+ (3 samples)
Sr	25	0.01-0.1% (all samples)
Sn	25*	
Ti	23	0.1%+ (1 sample)
Zn	23	0.1%+ (1 sample)

*trace amounts only

$$CaCO_3 + H^+ \longrightarrow Ca^{++} + DIC$$

where, DIC, the dissolved inorganic carbon, includes the species, $H_2CO_3^*$ ($CO_2 + H_2CO_3$), HCO_3^- and $CO_3^=$.

The dissolution reaction at the solid surface is influenced by the transfer of the reactants (e.g., hydrogen ion) to the interface and the products (calcium and DIC species) away from it. In addition, if the objective is to understand the effect of dissolution on the chemistry of the bulk solution, the rates of homogeneous reactions involving dissolution products in the solution and, if a gas phase is present, the rate of transport of inorganic carbon to or from the aqueous phase must be considered.

A schematic diagram illustrating the overall dissolution process in a system which includes a $CaCO_3$ solid phase, the aqueous solution and a gas phase which may contain carbon dioxide or may act as an infinite sink for CO_2 released from the aqueous phase is presented in Figure 2. The rate of change in bulk solution chemistry is affected by one or more of the reactions shown.

Reaction A in Figure 2 represents the decomposition of the solid phase, i.e., the net release of calcium and carbonate to the solution. This step might be a combination of reactant adsorption (e.g., H^+ or H_2O) on the $CaCO_3$ surface, chemical reaction with the surface and desorption of reaction products.

The rate of decomposition of the surface (and the rate of change in the bulk solution chemistry) may be controlled by the transport of hydrogen ions to the surface (reaction C) or the transport of reaction products (Ca^{++}, $CO_3^=$, HCO_3^-, and H_2CO_3) away from the surface (reaction B). If a gas phase is present, as shown in Figure 2, the bulk solution chemistry may be affected by the transport of reaction products or gas phase components to or from the bulk solution (reactions D and E). It is also possible, as indicated by reaction E, that a homogeneous solution phase reaction such as the protonation of the bicarbonate ion or the dehydration of carbon dioxide may effect the time varying chemical characteristics of the bulk solution and the solution within the boundary layers.

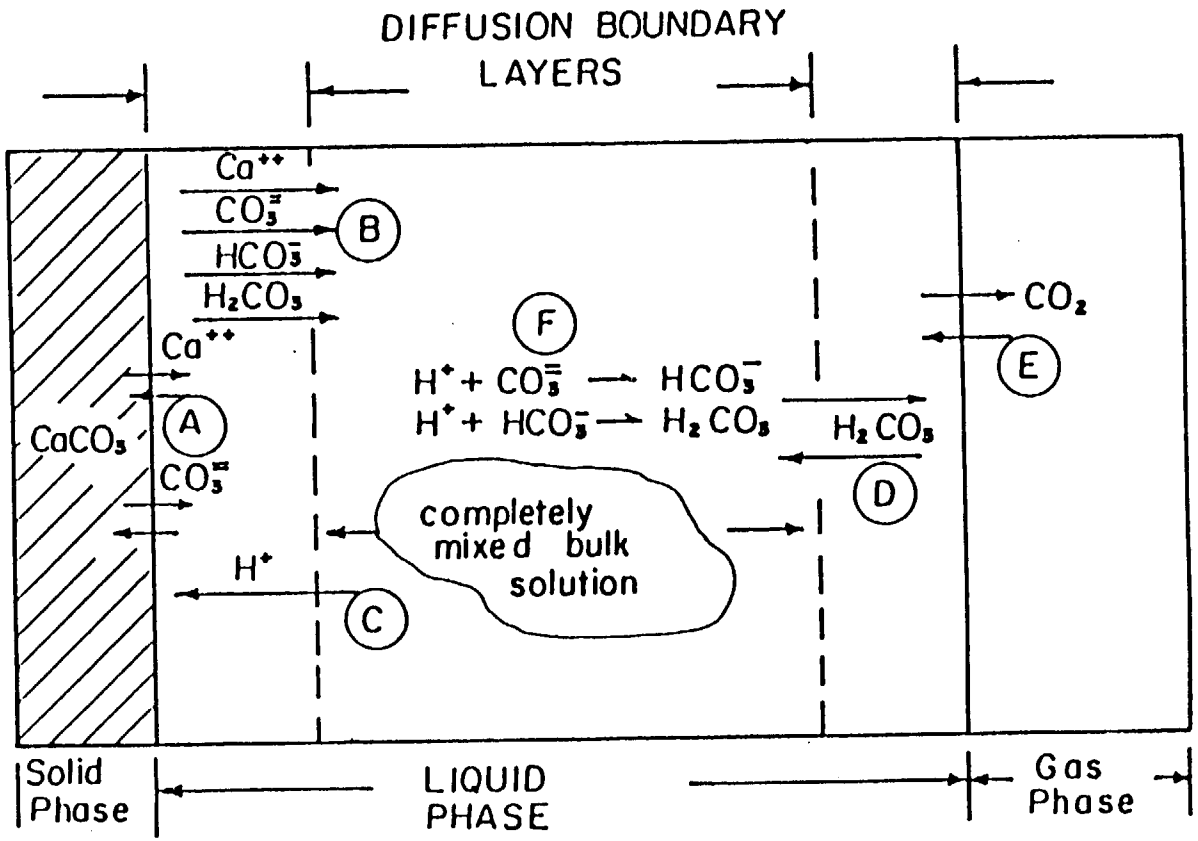

Figure 2. Schematic representation of the calcium carbonate dissolution process.

A significant amount of research has been conducted on mineral dissolution kinetics. The dissolution of calcite and limestone has been investigated for applications such as the formation of antacids (Lund et al., 1975), the neutralization of pickling acids (Eden and Truesdale, 1950; Gehm, 1944; Hoak et al., 1944, 1945, 1947; Reidl, 1947; Galloway and Colville, 1970), the neutralization of acid mine drainage (Pearson and McDonnell, 1975a, 1975b; Jarret, 1966, Mihok et al., 1968; Vatanatham, 1975), the effect of $CaCO_3$ sediments on the pH of sea water (Morse, 1978; Morse, 1974; Morse and Berner, 1972; Berner and Morse, 1974), the neutralization of CO_2-saturated waters (Frear and Johnson, 1929; Erga and Terjesen, 1956; Terjesen et al., 1961; Plummer et al., 1978; Plummer and Wigley, 1976), the neutralization of dilute acidic ground and surface waters (Bjerle and Rochelle, 1982, Vaillancourt, 1981; Sverdrup and Bjerle, 1982; Driscoll et al., 1982; Haddad, 1983), the neutralization of nitric acid solutions (Wentzler, 1971), sulfuric acid solutions (Vatanatham, 1975) and hydrochoric acid solutions (Lund et al., 1975; Tominaga, 1939).

It has been recognized for a long time that mass transport to or from the dissolving $CaCO_3$ surface has at least some effect on the kinetics of the process and therefore most recent, investigators have been careful to control (to some extent) the hydrodynamic conditions in their experimental reactor. A number of experimentors controlled the mixing intensity in mechanically agitated batch reactors containing suspensions of powdered calcite (Erga and Terjesen, 1956; Terjesen et al., 1961; Berner and Morse, 1974; Sjoberg, 1976; Sverdrup and Bjerle, 1982; Rickard and Sjoberg, 1983). Others have mounted rotating cylinders (King and Liu, 1933) or rotating disks (Wentzler, 1972; Lund et al., 1975; Rickard and Sjoberg, 1983; Sjoberg and Rickard, 1983) made of $CaCO_3$ in batch reactors. A few investigators have studied the dissolution reaction using flow-through packed-bed reactors (Pearson and KcDonnell, 1975a, 1975b; Vaillancourt, 1981; Haddad, 1983). In one case (Weyl, 1958) a fluid jet was directed against a calcite crystal.

In the cases where a batch reactor is used the rate of $CaCO_3$ dissolution is usually monitored by either a "pH stat" or "free drift" technique. The pH stat technique involves maintaining the bulk solution at a set-point pH by the controlled addition of mineral acid. The rate of $CaCO_3$ dissolution

is then related to the rate of hydrogen ion addition. The free drift technique involves measuring the pH and/or calcium ion concentration as a function of time as the suspended particles, rotating disk, etc. dissolve in the batch reactor.

Most batch reactor studies have been conducted using an "open" system, where the solution is in contact with a gas phase with a carbon dioxide partial pressure ranging from 0 to 100%. The packed column is usually operated as a closed system; inorganic carbon does not enter or leave the solution during the course of the dissolution reaction. The closed system is less complicated than the open system to model because, as noted in regard to Figure 2, the open system model may require an understanding of the rates of transport and reaction at the gas-solution interface (reactions D and E in Figure 2). There is no gas/liquid interface in an ideal closed system.

A review of the literature suggests that many investigators have recognized the complexity of the $CaCO_3$ dissolution process. Most have attempted to simplify the modeling of this process by delineating the rate limiting steps. It is, however, apparent that in making assumptions and interpretations of experimental data the various investigators have often been limited by the type of apparatus used and the experimental conditions. Consequently, it is difficult to generalize results.

Various processes have been proposed to regulate the dissolution of $CaCO_3$:

- The diffusion of hydrogen ion to the solid surface (King and Liu, 1933, Tominaga et al., 1939, Kaye, 1957, Gortikova and Panteeva, 1937, Neirode and Williams, 1971, Berner and Morse, 1974, Wentzler, 1972, Vaillancourt, 1981, Haddad, 1983).
- A heterogeneous "dissolution" reaction at the solid surface (Erga and Terjesen, 1956, Terjesen et al., 1961, Plummer and Wigley, 1976, Plummer et al., 1978, Berner and Morse, 1974, Sjoberg, 1976).
- Mixed kinetics in which transport and a heterogeneous reaction at the surface acting in series are important (Pearson and Mcdonnell, 1975, Rickard and Sjoberg, 1983, Lund et al., 1975, Berner and Morse, 1974, Plummer et al., 1978, 1976).
- The diffusion of reaction by-products, e.g. Ca^{++}, away from the solid surface (Weyl, 1958, Bjerle and Rocheele, 1982, Berner and Morse, 1974, Haddad, 1983).

- The dissolution and/or exsolution of carbon dioxide in or from the solution (Volpicelli et al., 1981).

Recent papers by Sjoberg and Rickard (Sjoberg and Rickard, 1983; Sjoberg and Rickard, 1984a; Sjoberg and Rickard, 1984b, Rickard and Sjoberg, 1983) provide a detailed analysis of the dissolution process. Sjoberg and Rickard used a rotating-disk/batch reactor apparatus and determined the initial rate of calcite dissolution using the pH-stat technique.

Rickard and Sjoberg (1983) concluded that in neutral to alkaline solutions at ambient temperature the dissolution of calcite was controlled by a mass transfer resistance and a surface reaction acting in series. In this scheme the observed rate of dissolution is a function of a transport rate, R_L, where

$$R_L = K_L (C_s - C_b) \tag{2}$$

and a first order surface reaction rate, R_c, where,

$$R_c = K_c (C_{eq} - C_s) \tag{3}$$

K_L and K_c are the mass transfer and surface reaction rate constants and C_s, C_b and C_{eq} are the molar calcium concentrations at the calcite surface, in the bulk solution and at equilibrium, respectively. The equations for R_L and R_c can be combined by assuming a steady state condition near the interface. The result is an expression for the overall rate of dissolution, R, i.e.,

$$R = K_o (C_{eq} - C_b) \tag{4}$$

where the overall rate constant, K_o, is given by

$$K_o = \frac{K_c K_L}{K_c + K_L} \quad . \tag{5}$$

According to Eq. (5), when $K_c >> K_L$ the dissolution rate is controlled by mass transfer and when $K_L >> K_c$ the surface reaction controls.

Rickard and Sjoberg (1983) concluded that at low pH the initial rate of calcite dissolution was controlled entirely by the rate of mass transfer of the hydrogen ion to the calcite surface. They determined that for pH < 4,

$$R = K_L' [H^+]_b^{0.9}, \quad (6)$$

where $[H^+]_b$ is the bulk solution hydrogen ion concentration and K_L' is an "apparent" mass transfer coefficient for the hydrogen ion. It is not clear exactly why Rickard and Sjoberg found it necessary to change from calcium ion transport control at neutral pH values and above to hydrogen ion transport at low pH. In any case, their assumptions and rate expression for low pH, Eq. (6), are generally consistent with low pH rate equations presented by a number of other investigators (Miadokova and Bednarova ; Lund et al., 1975; Berner and Morse, 1974; Plummer et al., 1975a; Nierode and Williams, 1971).

A plot from Sjoberg and Rickard (1984a) of the initial rate of calcite dissolution as a function of the bulk solution pH for a batch reactor/rotating disk/pH-stat system operating at 25°C and a disk rotational speed of 1000 rpm is presented in Figure 3. Note, the initial rate of dissolution was highest at low bulk solution pH. The rate decreased with increasing pH and approached a minimum (asymptotically) at pH > 5. Under the conditions used to obtain the data of Figure 3 the minimum initial rate of dissolution was approximately 6.3×10^{-10} moles calcium $cm^{-2}s^{-1}$. Sjoberg and Richard (1984a)concluded that the magnitude of this minimum rate was determined by both the mass transfer and surface reaction rate constants (Eq. 5).

Plummer et al. (1978) obtained the initial calcite dissolution rate as a function of the bulk solution pH. The results are presented in Figure 4. The pH-stat technique was used in conjunction with a mechanically agitated batch reactor containing crushed calcite (Iceland Spar). The CO_2 partial pressure was a controlled parameter and the temperature was 25°C.

The results plotted in Figure 4 are similar to those obtained by Sjoberg and Rickard, (1984a). As the bulk solution pH increased above pH = 4 the initial rate of dissolution asymptomatically approached a minimum value. The minimum rate (for $pCO_2 = 0.00$) was approximately 3×10^{-10} moles $cm^{-2}s^{-1}$.

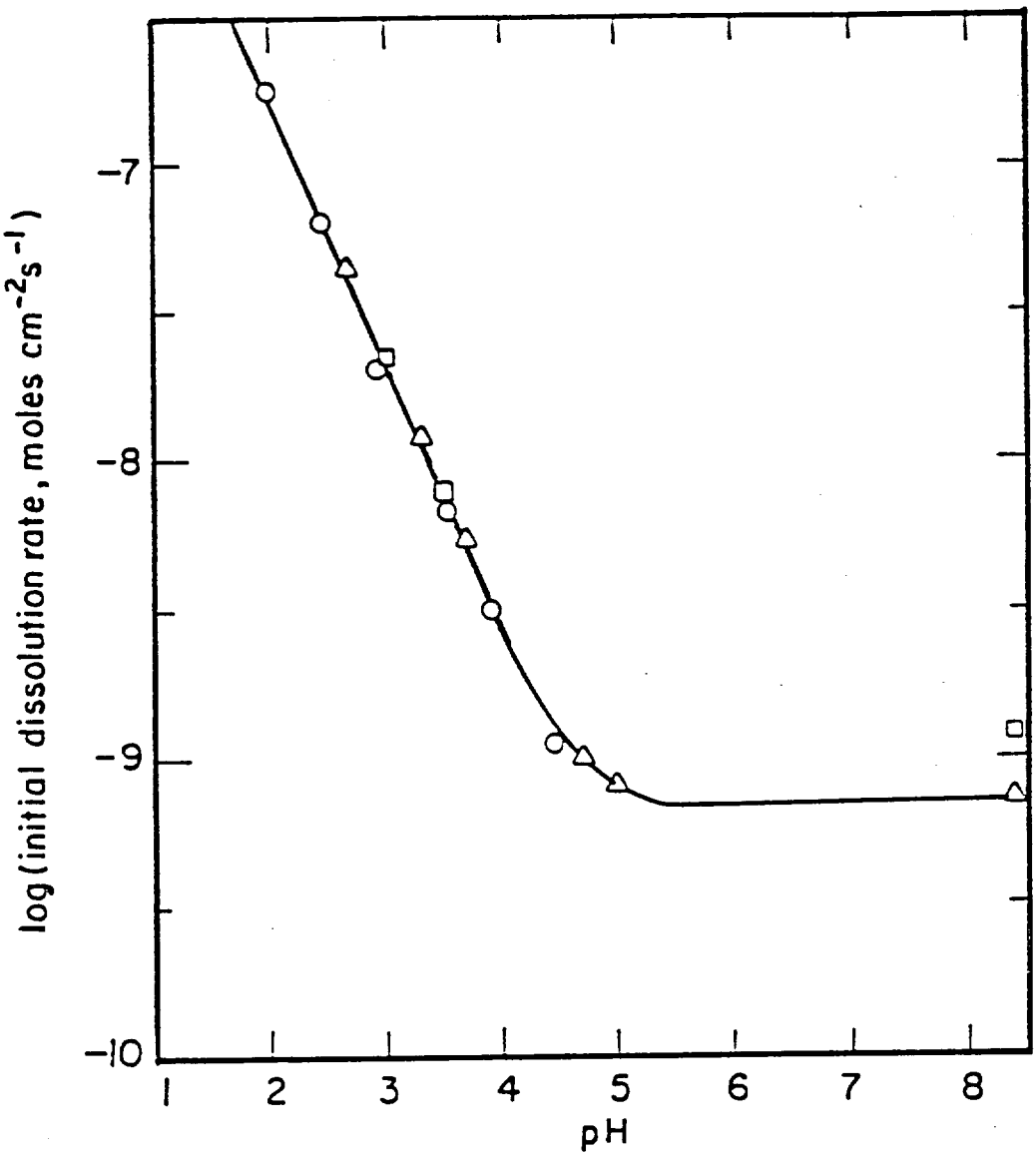

Figure 3. Initial rate of calcite dissolution as a function of the bulk solution pH from Sjoberg and Rickard (1984a). System was closed to atmospheric CO_2.

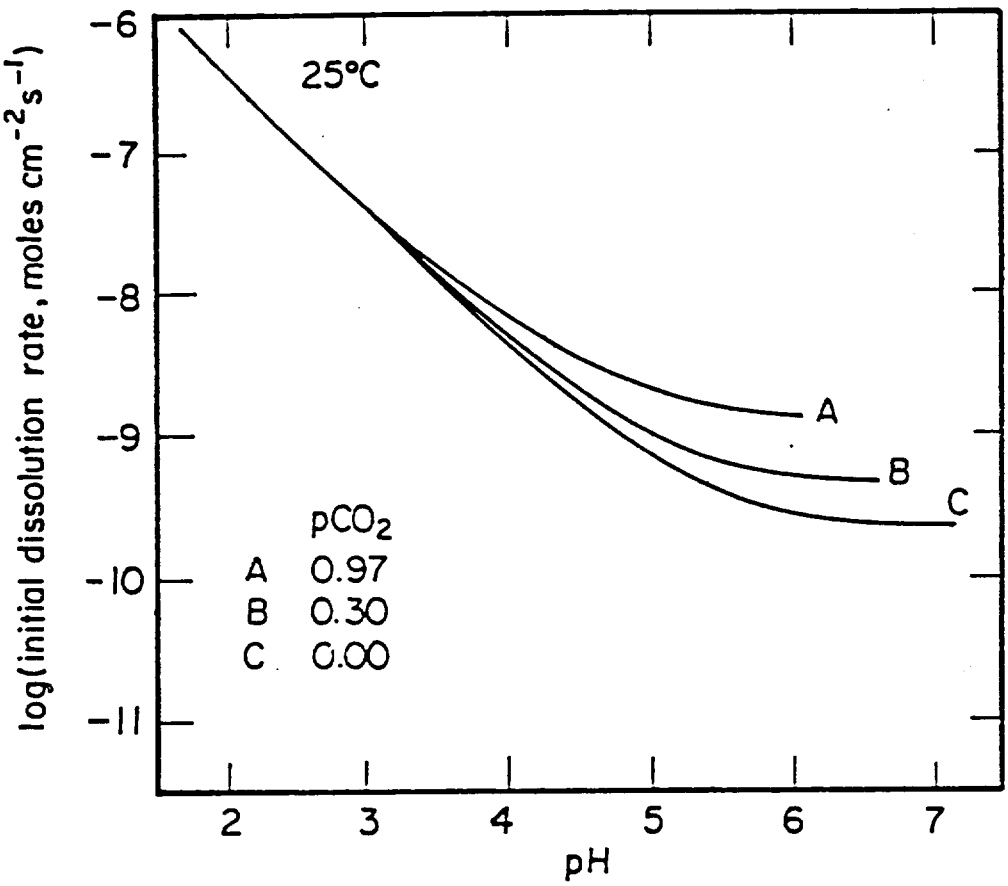

Figure 4. Initial rate of calcite dissolution as a function of bulk solution pH and partial pressure of carbon dioxide (Plummer et al., 1975).

Sjoberg and Rickard (1984b) plotted the initial rate of dissolution as a function of the square root of the disk rotational velocity, $\omega^{\frac{1}{2}}$, to illustrate the effect of the mass transfer coefficient, K_L, on the dissolution rate. An example for carrara marble, a bulk solution pH of 8.4, a background electrolyte of 0.7 M KCl and temperatures of 1 and 25°C is illustrated in Figure 5. In the rotating disk system K_L was directly proportional to $\omega^{\frac{1}{2}}$ and, therefore, if mass transfer was the controlling step, the dissolution rate, R, would be directly proportional to $\omega^{\frac{1}{2}}$. At a bulk solution pH of 8.4 the relationship between R and $\omega^{\frac{1}{2}}$ is linear only at low values of $\omega^{\frac{1}{2}}$. As $\omega^{\frac{1}{2}}$ increased, the surface reaction apparently became an increasingly important factor in determining the initial rate of dissolution.

For the results obtained at 25°C (Figure 5)) the relationship between R and $\omega^{\frac{1}{2}}$ was linear and mass transfer apparently controlled up to $\omega^{\frac{1}{2}} = 5\ s^{-1}$ where R was approximately equal to 7×10^{-10} moles $cm^{2-} s^{-1}$. At 1°C the effect of the surface reaction on R seemed to be even greater than at 25°C. The upper limit for mass transfer control was $R \simeq 1 \times 10^{-10}$ moles $cm^{-2}s^{-1}$ at $\omega^{\frac{1}{2}} = 2\ s^{-1}$.

It will be indicated in a subsequent section that in packed bed limestone contactors operated under the conditions used in this study, the maximum rate of dissolution for bulk solution pH values greater than 4 is generally less than 1×10^{-10} moles $cm^{-2}s^{-1}$. It therefore seems reasonable to assume that, based on Sjoberg and Rickard's results (Figure 3)), the rate of transport of calcium ion away from the interface controlled the dissolution rate throughout the entire depth of the packed columns used in this study.

It has been shown that the presence of certain substances can reduce the rate of calcite dissolution. This effect has been noted for ferric and chromic ions, (King and Liu, 1933), copper (Erga and Terjesen, 1956), aluminum (Volpicelli et al., 1981), scandium (Nestaas and Terjesen, 1969), organic matter, magnesium and orthophosphate (Morse 1974a, 1974b; Berner and Morse, 1974). The effect of contaminants on the rate of dissolution can be significant at very low contaminant concentrations. Nestaas and Terjesen (1969) concluded that metal ions adsorb at active spots or kinks on the surface of the dissolving crystal, blocking the dissolution process at that location. At the present time there are no methods available for quantifying the effect of contaminants

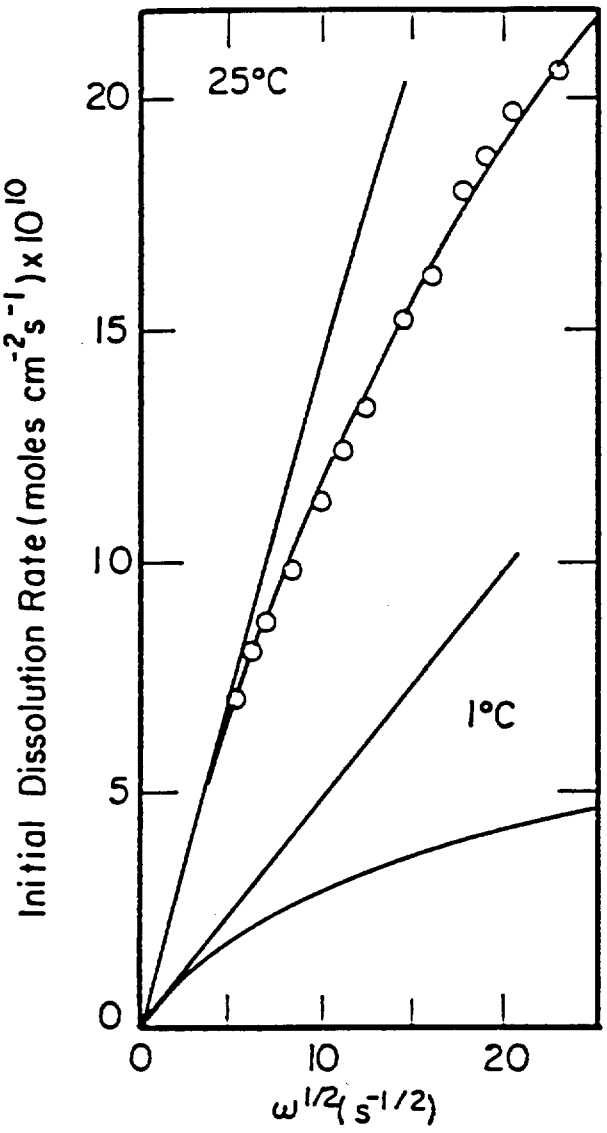

Figure 5. Initial rate of calcite dissolution as a function of the square root of the rotating disk rotational speed. Bulk solution pH was constant at 8.4 and the system was closed to atmospheric CO_2 (Sjoberg and Rickard, 1984b).

on the dissolution rate, particularly the dissolution rate of limestone. Eventually, for example, relationships between the contaminant concentration and K_c, the surface reaction constant, may be developed.

PACKED-BED REACTORS

Only a few studies have involved attempts to model the kinetics of limestone dissolution in continuous flow, packed-bed reactors (Pearson and McDonnell,1975a, 1975b; Barton and Vatanatham, 1976; and Vaillancourt, 1981).

Pearson and McDonnell (1975a, 1975b) studied the neutralization of acidic drainage from coal mines using packed columns and in-stream barriers of large (6.4 to 10 cm. effective diameter) limestone particles. Their open-to-the-atmosphere experiments were conducted at ambient temperature and in the presence and absence of dissolved metal ions.

Pearson and McDonnell (1975a) indicated that a rate equation based on hydrogen ion transport coupled with a surface reaction can be used to describe limestone dissolution kinetics. The proposed model is given by:

$$\frac{V}{A}\frac{dC_o}{dt} = K C_o^{n'} = K_a C_i^{n} = K_d (C_o - C_i) \qquad (7)$$

where V/A is the inverse of the interfacial area per unit volume of fluid in the column, K is an overall rate constant, K_a is a surface reaction rate constant, K_d is the mass transfer coefficient, C_o is the hydrogen ion concentration in the bulk solution, C_i is the hydrogen ion concentration at the limestone/water interface and n' and n are exponents.

Pearson and McDonnell (1975a, 1975b) did not use their experimental data to test the proposed rate equation, Eq. 7, but instead developed an empirical expression which related the rate of limestone dissolution to water temperature, pH, solution ionic strength, the bicarbonate ion concentration and the hydraulic shear stress. Their overall model included an expression for predicting the rate of CO_2 exolution at the air/water interface above the packed bed. The experimental conditions used by Pearson and McDonnell (1975a) to develop their empirical equations are appropriate for the treatment

of acidic drainage from coal mines but not the dilute acidic surface waters used as potable supplies.

Two groups of investigators, Barton and Vatanatham (1976) and Vaillancourt (1981) assumed that the rate of limestone dissolution in closed and open-to-the atmosphere, packed-columns is controlled by the rate of hydrogen ion transport from the bulk solution to the limestone surface. Vaillancourt (1981) used the conventional relationship,

$$\frac{U_s}{\varepsilon}\frac{dH_b^+}{dx} = -K\ a\ (H_b^+ - H_{eq}^+) \qquad (8)$$

where U_s is the superficial velocity, ε is the bed porosity, K is the mass transfer coefficient for hydrogen ion, a is the surface area of limestone per unit volume of interstitial water, x is distance in the axial direction, H_b^+ is the hydrogen ion concentration in the bulk solution and H_{eq}^+ is the hydrogen ion concentration when the solution and limestone solid phase are at equilibrium (under a closed-to-the-atmosphere condition). Vaillancourt (1981) correlated experimentally determined mass transfer coefficients with the limestone particle diameter, superficial velocity and fluid properties using dimensionless parameters.

Unfortunately, Vaillancourt (1981) used very short packed-columns with high Reynolds numbers in his experiments and did not consider the adverse effect these conditions had on his assumption of plug flow. He also did not consider the effect of raw water chemistry on the magnitude of H_{eq}^+. A constant value was incorrectly used for all solutions studied.

Vatanatham (1975) and Barton and Vatanatham (1976) studied the kinetics of limestone dissolution in acidic solutions using an open-to-the-atmosphere batch reactor and a recycle-downflow, packed-bed reactor system. Several models were tested including, zero order reaction controls, carbon dioxide transport controls, surface reaction controls and hydrogen ion transport controls. Barton and Vatanatham (1976) concluded that in the pH range of 2 to 6 hydrogen ion transport controls. They did not determine the rate limiting step outside this range but assumed that the lack of agreement between the experimental data and the hydrogen ion transport model was due to experimental error or the increasing importance of other transport or rate limiting mechanisms.

The kinetic equation used by Barton and Vatanatham (1976) for pH values between 2 and 6 is given by,

$$\frac{dW}{dt} W^{-2/3} = \frac{k\ M\ W_o}{6\ \rho\ D_o} [H_b^+ - H_{eq}^+], \qquad (9)$$

where W and W_o are the mols of $CaCO_3$ present at any time, t, and at t = 0, M is the molecular weight of $CaCO_3$, D_o is the initial diameter of the limestone particles, ρ is the mass density of limestone, H_{eq}^+ is the hydrogen ion concentration in the bulk solution at equilibrium and H_b^+ is the hydrogen ion concentration in the bulk solution at any time. Eq. 9 is essentially a first order (film) transport equation modified to include the change in interfacial area as the particles dissolve and decrease in size. Unfortunately Barton and Vatanatham (1976) made an error in deriving Eq. 9. The number six should appear in the numerator and not in the denominator and therefore all their model calculated results were in error by a factor of 36.

METAL RELEASE FROM PIPES

There is considerable concern over the corrosion of water distribution systems. Elevated corrosion rates may substantially reduce the service period of piping systems resulting in increased operation and maintenance expenses (Anderson and Berry, 1981). Metal release from water distribution systems may also cause water supplies to exceed the U.S. Environmental Protection Agency (U.S. EPA) Standards for maximum contaminant levels (MCL) or secondary maximum contaminant levels (SMCL). Maximum contaminant levels (MCL) are established for concentrations of compounds that may result in human health problems, while SMCL are primarily established for esthetic criteria.

Metal release may occur from copper, galvanized steel, iron and lead pipes, and from lead-tin solder coated on copper piping materials. Human health concerns are largely associated with the leaching of lead from lead pipe or lead-tin solder coated on copper pipe. The toxic effects of lead are well established (NAS 1977; Waldbott, 1978). Lead is an active and cumulative toxicant which alters neurological and metabolic functions. It has been associated with hyperactivity, hypertension, mental retardation and motor disfunctions (NAS 1977; Patterson and O'Brien, 1979). Several studies

have established a link between high concentrations of lead in drinking water, and elevated concentrations of lead in blood and subsequent health problems (Beeners et al, 1976; Campbell et al., 1977; Cameron and Wunderlich, 1976). Because of human health concerns, the U.S. EPA established a MCL for lead of 0.05 mg $Pb \cdot L^{-1}$.

Although copper is an essential trace metal, at elevated concentrations it has been implicated as a gastrointestinal poison (Doull et al., 1980). The U.S. EPA Secondary MCL for copper is 1.0 mg $Cu \cdot L^{-1}$. This standard has largely been established for esthetic considerations, such as the taste and staining characteristics associated with elevated concentrations.

Elevated corrosion rates have been reported for a number of regions (Hudson and Gilcreas, 1976; Dansel, 1976; Patterson and O'Brien, 1979; Karalekas, et al., 1983; Maessen et al., 1985). Of particular concern are soft-water supplies such as in the northeastern, southeastern and northwestern United States (Patterson and O'Brien, 1979).

Corrosion is a deterioration of a metal which usually occurs as a result of an electrochemical reaction. For corrosion to occur, an electrochemical cell must be established including an anode, a cathode, an electrolyte solution, and an electrical (metal) connection between the anode and cathode. As an electrochemical reaction proceeds oxidation occurs at the anode releasing electrons which are transmitted through the electrical connection to the cathode. These electrons are accepted at the cathode through a reduction reaction. The tendency for a metal to oxidize (and subsequently exhibit corrosion) is measured through its oxidation potential (E°). Some values of oxidation potential for some relevant reactions are summarized in Table 4. Note the reaction with the highest oxidation potential will have the greatest tendency to undergo oxidation in an electrochemical reaction. For example, if copper and lead form an electrochemical cell at a copper-lead solder joint, lead would be oxidized (corroded) while copper would be reduced by virtue of their values of oxidation potential.

There are two conditions by which corrosion may be restricted. First, the electrochemical (redox) potential and pH may not thermodynamically favor oxidation. This condition is termed immunity. The second condition involves the formation of a sparingly soluble solid phase with an oxidation by-product,

TABLE 4 Oxidation Potential of Metallic Materials

Anode	Anodic Reactions	Potential E° (volts)
Zinc	$Zn(s) \rightarrow Zn^{2+} + 2e^-$	0.76
Iron Soft Solder	$Fe(s) \rightarrow Fe^{2+} + 2e^-$	0.44
Tin	$Sn(s) \rightarrow Sn^{2} + 2e^-$	0.136
Lead	$Pb(s) \rightarrow Pb^{2+} + 2e^-$	0.126
Copper	$Cu(s) \rightarrow Cu^{2+} + 2e^-$	-0.345

such as an oxide, hydroxide or salt. If this solid adheres as a film on the metal surface, then it may mitigate corrosion. This process is referred to as passivation. The effectiveness of passivation films is highly variable, and depends on the affinity of the solid phase for the metal and whether coverage is complete or partial.

Hilburn (1983) developed two conceptual models for uniform corrosion. The direct-dissolution model is applicable when the metal is oxidized and directly released to solution. Under these conditions the corrosion rate is controlled by either the kinetics of the reaction, or the transport of reactants and products to and from the metal surface through solution. The dissolution-and-film-growth-model applies to metals which form a passivation film. The overall corrosion rate may be regulated by reaction kinetics, transport through the passivation film or solution transport, whichever is the rate-limiting process.

Corrosion is an extremely complicated process. For example factors such as pipe age, pipe length, impurities in the pipe material, interval of solder joints, temperature, turbulence and water chemistry can all contribute to corrosion (Herrera et al., 1982; Hilburn, 1983, 1983; Schock, 1984; Maesson et al., 1985; Treweek et al., 1985). As a result, it is often difficult to evaluate factors regulating metal release from piping systems. Maessen et al. (1984) studied metal mobilization in home well-water systems in Nova Scotia. They assessed bedrock type (e.g. granite, limestone), proximity to the coast, well-type (e.g. dug, drilled) and depth, plumbing data (e.g. length of piping, age of piping, type of piping), as well as solution chemistry on the extent of metal release from water distribution systems. They found significant leaching of copper, lead and zinc occurred in some systems. Concentrations of metals were elevated in water that had been in contact with piping material for a prolonged periods of time (e.g. overnight, standing) relative to running water samples. Although a wide range of bedrock, water chemistry and plumbing conditions were evaluated, no factor could be found to systematically predict the extent of metal leaching. Moreover, indexes commonly used to assess the corrosive tendency of a water (Langelier, Ryznar, Aggressiveness indexes, and the ratio of SO_4^{2} and Cl^{-1} to alkalinity) and pH were poor predictors of metal release.

Meranger et al. (1983) evaluated metal leaching from cottage piping systems that contacted acidic lakewater in northern Ontario. They found elevated leaching of cadmium, copper, lead and zinc. Mobilization rates were greatest during the first two hours of contact time with the pipe, but concentrations continued to increase for a period of up to 10 days. Highest metal concentrations were again obtained with the first sample collected and concentrations decreased by up to 97% in the third liter of water collected. Although the authors were concerned that acidic deposition to the region resulted in surface water acidification and enhanced the corrosivity of lake water, because these waters are naturally soft and corrosive this effect is not clear.

Although it is often difficult to interpret field data because of all the physical and chemical factors which contribute to corrosion, considerable progress has been made in recent years through controlled laboratory experiments in evaluating the chemistry of passivation films and processes regulating the formation of films. Housing and building systems frequently have sections of pipe that remain stagnant for prolonged periods of time. Initially metal release is regulated by mass-transport reactions, however over time concentrations can approach and reach saturation with respect to mineral phase solubility (Schock, 1984). Therefore, solubility calculations may be used as worst-case assessment of metal leaching.

In recent years thermodynamic calculations have been used as a tool to assess trace metal chemistry and the stability of passivation films within water distribution systems. Several types of passivation films may form on metal pipe depending on the chemical characteristics of the water supply (Table 5). Patterson and O'Brien (1979) discussed the role of inorganic carbon in regulating the release of lead from lead pipe. Using thermodynamic calculations, they found that the solubility of lead decreases with increasing inorganic carbon concentrations. Moreover, they suggested that elevated inorganic carbon concentrations result in the formation of an insoluble lead carbonate passivation film. This film not only reduces lead solubility but also strongly adheres to the pipe surface, limiting the release of particulate lead to water. Their calculations suggest that reduced inorganic carbon

TABLE 5

Passivation film minerals that may be important in regulating metal solubility in water distribution systems

COMPOUND	STOICHIOMETRY
Lead Pipe	
Lead hydroxide	$Pb(OH)_2$
Lead carbonate (cerussite)	$Pb\ CO_3$
Basic lead carbonate (hydrocerussite)	$Pb_3(CO_3)_2(OH)_2$
Lead Sulfate	$Pb\ SO_4$
Copper Pipe	
Copper hydroxide	$Cu(OH)_2$
Copper carbonate	$CuCO_3$
Basic copper carbonate (malachite)	$Cu_2(OH)_2CO_3$
Basic copper carbonate (azurite)	$Cu_3(OH)_2(CO_3)_2$
Copper sulfate	$CuSO_4$
Basic copper sulfate(brochantite)	$Cu_4(OH)_6SO_4$
Basic copper chloride(atacamite)	$Cu_2(OH)_2Cl$
Galvanized Steel Pipe	
Zinc hydroxide	$Zn(OH)_2$
Zinc carbonate	$ZnCO_3$
Basic zinc carbonate(hydrozincite)	$Zn_5(OH)_6(CO_3)_2$
Zinc sulfate	$ZnSO_4$
Basic zinc silicate(hemimorphite)	$Zn_4\ Si_2\ O_7(OH)_2 \cdot H_2O$

concentrations facilitate the formation of a lead hydroxide film which does not adhere strongly to the pipe surface and periodically is released to the water supply as particulate lead.

In a series of papers, Schock (1980), Schock and Gardels (1983), and Schock (1984) greatly elaborate on the role of inorganic carbon in controlling trace metal concentrations in water distribution systems. Schock (1980) suggested that the thermodynamic analysis by Patterson and O'Brien (1979) was incorrect due to a failure to consider soluble lead-carbonate complexes. Lead forms strong aqueous complexes with carbonate and therefore elevated dissolved inorganic carbon concentrations can significantly enhance aqueous lead concentrations. As a result, the contention by Patterson and O'Brien (1979) that increases in dissolved inorganic carbon concentration reduce aqueous lead concentrations is incorrect and may suggest counter-productive water treatment strategies.

Due to the relatively high solubility of lead at low pH and the potential to form lead-carbonate complexes at higher pH values the conditions under which the theoretical solubility of lead is below the U.S. EPA MCL of 0.05 mg $Pb \cdot L^{-1}$ are limited to relatively high pH values (8.0 - 10) and low dissolved inorganic carbon concentrations. Schock (1984) indicated that under these conditions the concentrations of lead would be generally regulated by the solubility of hydrocerussite ($Pb_3(CO_3)_2(OH_2)$), a tightly adhering passivation film. These conditions would limit the release of particulate lead to water supplies.

In addition to lead solubility, Schock (1984) evaluated the theoretical solubility of passivation films from copper and galvanized steel pipe. Because both zinc and copper are hydrolyzing metals and form soluble complexes with carbonate, it is reasonable to expect their solubility to mimic lead. Copper exhibits a considerable variation in solubility over a range of pH and dissolved inorganic carbon concentrations. Generally the solubility of copper in the pH range 7 to 11 is well below the U.S. EPA secondary MCL of 1 mg $Cu \cdot L^{-1}$. It is, therefore not as difficult to meet the U.S. EPA secondary MCL for copper as it is to meet the MCL for lead. Like lead, the minimum theoretical solubility occurs at elevated pH values (9-10) and the solubility is enhanced at high pH values due to the formation of soluble carbonate com-

plexes. Schock (1984) indicates that in the pH range of 9-10 the theoretical solubility of copper is regulated by tenorite (CuO).

The theoretical solubility of zinc has a minimum value near pH 9 and in this pH range is thought to be regulated by the solubility of hydrozincite ($Zn_5(CO_3)_2(OH)_6$) (Schock 1984). Hydrozincite is not a strongly adhering passivation film. Therefore, zinc concentrations in water supplies using galvanized steel pipe may be significantly enhanced by the release of particulate Zn. Unlike lead and to a lesser extent copper, zinc does not form strong soluble complexes with carbonate. Therefore, pH is the major factor regulating variations in the solubility of dissolved zinc from galvanized steel pipe. However within the pH range 7 to 11, the theoretical solubility of dissolved zinc is well below the USEPA SMCL of 5 mg $Zn \cdot L^{-1}$ (Schock 1984).

While thermodynamic calculations represent an important tool to assess trace metal solubility and the stability of passivation films, they clearly have many limitations. As indicated previously, thermodynamic calculations should be viewed as an upper-limit of dissolved metal concentrations. Under many conditions, particularly when water has been in contact with piping material for a short period of time, the release of corrosion by-products will be controlled by mass-transport reactions. Physical factors such as the poor adherence of passivation films to piping material and/or erosion of these films due to turbulance can significantly increase metal concentrations through the release of particulate metal. Moreover, our understanding of the temperature dependence (standard enthalpy values) of metal complexation and solubility reactions is limited. So it is difficult to make thermodynamic solubility calculations at temperatures other than 25°C with confidence. Finally, while thermodynamic calculations provide theoretical values of dissolved metal concentration which may be useful in evaluating compliance with U.S. EPA drinking water standards, no information is obtained on the destruction of the metal pipe. While an insoluble passivation film may restrict the release of metal to solution, if it is not impervious to molecular oxygen then oxidation may continue and substantially diminish the lifetime of the metallic piping material.